

Genetic-guided GFlowNets: Advancing in Practical Molecular Optimization Benchmark

Hyeonah Kim¹ Minsu Kim¹ Sanghyeok Choi¹ Jinkyoo Park¹

Abstract

This paper proposes a novel variant of GFlowNet, genetic-guided GFlowNet (Genetic GFN), which integrates an iterative genetic search into GFlowNet. Genetic search effectively guides the GFlowNet to high-rewarded regions, addressing global over-exploration that results in training inefficiency and exploring limited regions. In addition, training strategies, such as rank-based replay training and unsupervised maximum likelihood pre-training, are further introduced to improve the sample efficiency of Genetic GFN. The proposed method shows a *state-of-the-art* score of 16.213, significantly outperforming the reported best score in the benchmark of 15.185, in practical molecular optimization (PMO), which is an official benchmark for sample-efficient molecular optimization. Remarkably, ours exceeds all baselines, including reinforcement learning, Bayesian optimization, generative models, GFlowNets, and genetic algorithms, in 14 out of 23 tasks. Our code is available at https://github.com/hyeonahkimm/genetic_gfn.

1. Introduction

Discovering new molecules is one of the fundamental tasks in the chemical domains with applications such as drug discovery (Hughes et al., 2011) and material design (Yan et al., 2018). Especially, *de novo* molecular optimization aims to generate a new molecule from scratch to achieve the desired property. Numerous studies have made significant progress using various approaches, including Bayesian optimization (e.g., Tripp et al., 2021), reinforcement learning (e.g., Olivecrona et al., 2017), latent optimization with variational autoencoders (e.g., Gómez-Bombarelli et al., 2018), generative flow networks (e.g., Bengio et al., 2021b), and

¹Department of Industrial & Systems Engineering, Korea Advanced Institute of Science and Technology (KAIST), Daejeon, South Korea.. Correspondence to: Hyeonah Kim <hyeonah_kim@kaist.ac.kr>.

Under review.

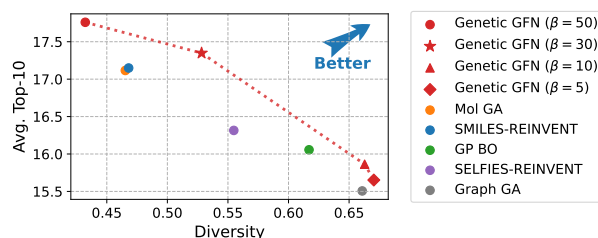


Figure 1. A trade-off between scores (y-axis) and diversity (x-axis) in the practical molecular optimization (PMO) benchmark (Gao et al., 2022a). The average scores of Top-10 and the diversity of Top-100 are illustrated.

genetic algorithms (e.g., Jensen, 2019).

The recent work of Gao et al. (2022a) proposes a practical molecular optimization (PMO) benchmark, emphasizing the importance of sample efficiency in *de novo* molecular optimization for practical applicability. The benchmark is reasonable because real-world applications of molecule optimization (e.g., drug discovery) require expensive scoring processes such as wet lab experiments. The PMO benchmark evaluates a range of methodologies, including deep reinforcement learning, genetic algorithms, and Bayesian optimization, under the constraints of a finite oracle budget, i.e., the number of evaluations.

Interestingly, we found a pronounced trade-off between attaining high evaluation scores within a limited budget and generating diverse molecular candidates, as highlighted in Figure 1. This observation indicates that excessively prioritizing diversity can compromise the efficiency of the optimization process. For example, a generative flow network (GFlowNet or GFN; Bengio et al., 2021b), which serves as a promising generator for sampling diverse candidates, faces challenges in the benchmark.

Another interesting observation is that the classical evolutionary search algorithms, like genetic algorithms (GA), still demonstrate their compatibility compared to recently proposed deep learning methods. We conjecture that their high sample efficiency stems from a powerful genetic operator focusing on high-scoring (but restricted) regions. Specifically, the GA evolves a population, a set of candidates of the

current generation, using genetic operators recombining candidates. This approach enables the algorithm to explore the focused regions effectively by refining the current samples to higher-rewarded ones in the vast combinatorial space. It is noteworthy that their optimization capability also derives from the sophisticated design of genetic operations established by extensive domain knowledge (Yoshikawa et al., 2018; Jensen, 2019; Polishchuk, 2020; Ahn et al., 2020; Tripp & Hernández-Lobato, 2023).

Based on these observations, this work proposes a new variant of GFlowNet, genetic-guided GFlowNets (Genetic GFN), by integrating the strengths of both GFlowNets and GA. The primary objective of the proposed method is to leverage the diversified global search capability of GFlowNets and the potent optimization capabilities of genetic algorithms, synergizing them for sample-efficient molecular optimization.

In detail, we first parameterize the generator into a string-based sequential model, which is pre-trained on unlabelled chemical data to maximize the likelihood of valid molecules. Then, we fine-tuned the pre-trained model to maximize a specific score function by minimizing a trajectory balance loss (Malkin et al., 2022), a training loss for GFlowNets. To guide our policy towards regions with high rewards, two components are introduced: genetic search and reweighted replay training. The genetic search component generates various offspring samples through crossover and mutation processes. Additionally, rank-based sampling (Tripp et al., 2020) is employed not only in selecting the GA population but also in sampling the training batch. Lastly, to constrain our generative model to produce a realistic, valid chemical structure, we use the KL divergence between the pre-trained and fine-tuning models as a regularizer.

Extensive experiments demonstrate our remarkable performance, achieving the highest total score of 16.213 across 23 oracles. This surpasses the state-of-the-art RL method, REINVENT, with 15.185, and the GA method, Mol GA, with 15.686, outperforming 24 other baselines within the benchmark. The results show that Genetic GFN enables the parameterization of the distribution across the entire molecular space through genetic-guided high-reward search. Moreover, Genetic GFN demonstrates the controllability to trade-off between optimization capability and diversity using the inverse temperature β . As a result, ours achieves an enhanced performance of 15.815, surpassing REINVENT (0.468) and Mol GA (0.465) in diversity with 0.528.

2. Preliminary

2.1. Practical Molecular Optimization

The practical molecular optimization (PMO) benchmark is suggested to provide a unified and practical experimental

protocol for molecular design (Gao et al., 2022a). The goal is to maximize the molecule score \mathcal{O} , called oracle, which reflects how well a molecule satisfies the required property. Formally, it can be formulated as follows:

$$x^* = \arg \max_{x \in \mathcal{X}} \mathcal{O}(x),$$

where x is a molecule, and \mathcal{X} denotes the chemical space which comprises all possible molecules.

The PMO benchmark employs 23 widely-used oracle functions based on the existing benchmarks such as GuacaMol (Brown et al., 2019) and Therapeutics Data Commons (TDC; Huang et al., 2021). In particular, DRD2 (Olivecrona et al., 2017), GSK3 β , and JNK3 (Li et al., 2018) represent machine learning models that predict bioactivities relevant to their corresponding disease targets, while QED (Bickerton et al., 2012) measures drug safety with a relatively simple function. Oracles from GuacaMol are designed to emulate objectives pertinent to drug discovery, encompassing multi-property objective functions as well as measures of similarity or dissimilarity to target molecules. Every oracle function is normalized from 0 to 1.

To consider both optimization ability and sample efficiency, they limit the number of oracle calls to 10,000 and measure the area under the curve (AUC). They also provide various performance metrics, including Top- K average scores, diversity, and synthetic accessibility (SA) scores. In the PMO benchmark, an ideal algorithm is characterized by strong optimality ability, sample efficiency, generalization to oracle functions, and robustness to random seeds and hyperparameters. The authors adopted 25 baselines across the various molecular assembly strategies and optimization algorithms. They compared performance with the consistent experimental setting, e.g., the same dataset for the pre-training.

2.2. Generative Flow Networks

Generative Flow Networks, or GFlowNets (Bengio et al., 2021b), are amortized inference methods that draw samples from the target energy distribution. A GFlowNet is formulated as a Markov decision process (MDP) where the target distribution $P(x) = e^{-\mathcal{E}(x)}/Z$ is defined on the combinatorial solution space \mathcal{X} , where $Z = \sum_{x \in \mathcal{X}} e^{-\mathcal{E}(x)}$. However, the partition function Z is intractable, so we only have an unnormalized target distribution called *reward* $R(x) = e^{-\mathcal{E}(x)}$. GFlowNets follow a constructive generative process, iteratively modifying a state with discrete *actions*; we define trajectory as a sequence of states $\tau = (s_0, \dots, s_T)$. Since $R(x)$ is defined on the terminal state $s_T = x$, GFlowNet training can be seen as episodic reinforcement learning, where the reward is only observed in the terminal state.

A GFlowNet models flow F of particles along a pointed directed acyclic graph (DAG). The source point of DAG

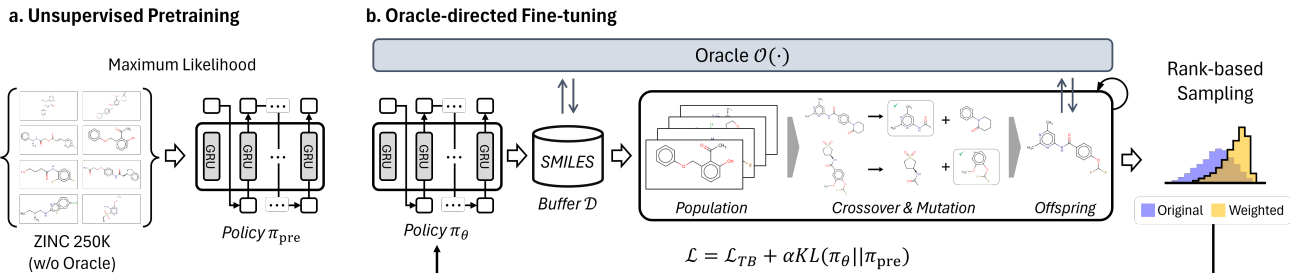


Figure 2. Overview of Genetic GFN.

is the initial state s_0 , and each sink node of DAG is the terminal state s_T . The *trajectory flow* $F(\tau)$ is the amount of particles that flow through the trajectory τ . The *state flow* $F(s)$ is defined as the sum of trajectory flows where the trajectory includes the state: $F(s) = \sum_{s \in \tau} F(\tau)$. The *edge flow* $F(s \rightarrow s')$ is the sum of trajectory flows where the trajectory includes subsequence of two state s, s' : $F(s \rightarrow s') = \sum_{(s, s') \in \tau} F(\tau)$.

Given flow function F , we can derive two policy distributions. First, *forward policy* $P_F(s'|s)$ which is the probability of moving from the current state s to its child state s' is defined edge flow $F(s \rightarrow s')$ denominated by current state flow $F(s)$, i.e., $P_F(s'|s) = F(s \rightarrow s')/F(s)$. Similarly, *backward policy* $P_B(s|s')$, which is the probability of moving from the current state s' to its parent state s , is defined as $P_B(s|s') = F(s \rightarrow s')/F(s')$. Using this two policy we can derive an optimal sampler $P(s_T) = \prod P_F(s_t|s_{t-1}) = R(s_T)/Z$ if the GFlowNet satisfies some of balance condition (Bengio et al., 2021a; Jain et al., 2022; Malkin et al., 2022; Madan et al., 2023; Pan et al., 2023; Shen et al., 2023).

Trajectory balance loss (Malkin et al., 2022). One of the most popular conditions is *trajectory balance (TB)*, which directly parameterizes P_F , P_B , and flow of initial state (i.e., partition function) Z to satisfies follows:

$$Z \prod_{t=1}^n P_F(s_t|s_{t-1}) = R(s_T) \prod_{t=1}^n P_B(s_{t-1}|s_t),$$

Then, this trajectory balance equation is converted into a loss function to be minimized along sampled trajectories.

$$\mathcal{L}_{TB}(\tau; \theta) = \left(\log \frac{Z_\theta \prod_{t=1}^n P_F(s_t|s_{t-1}; \theta)}{R(x) \prod_{t=1}^n P_B(s_{t-1}|s_t)} \right)^2 \quad (1)$$

In GFlowNet training, employing exploratory behavior policies or replay training is allowed since GFlowNet can be trained in an off-policy manner, which is a key advantage (Bengio et al., 2021b; Malkin et al., 2022; Zimmermann et al., 2023; Kim et al., 2023d).

3. Genetic-guided GFlowNet

Our proposed approach, genetic-guided GFlowNet (Genetic GFN), is developed based on insights from the PMO benchmark. As detailed in the subsequent sections, our methodology involves an initial unsupervised pre-training phase, where the model is trained on a chemical dataset to generate valid molecules. Subsequently, the model is tuned to maximize a specific oracle function value. In oracle-directed fine-tuning, we train the model to minimize the trajectory balance loss by sampling from the rank-based reweighted dataset. To address the over-exploration for low-rewarded regions, we integrate genetic algorithms into GFlowNet fine-tuning. The genetic search explores high-reward regions, which are hard to find using the current generative policy only. As a last component, we introduce a penalty for the KL divergence from the pre-trained model to ensure the model does not deviate excessively from the pre-trained model, thus still producing valid molecules. The overall procedure is illustrated in Figure 2.

3.1. Pre-training a String-based Generative Policy

Motivated by REINVENT (Olivecrona et al., 2017), we adopt a sequence generative policy using a string-based assembly strategy. Specifically, we employ the simplified molecular-input line-entry system (SMILES; Weininger, 1988) format and parameterize the policy using a recurrent neural network architecture (Chung et al., 2014). Then, the probability of generating a molecule, $\pi_\theta(\mathbf{x})$, can be factorized to $\prod_{t=1}^n \pi_\theta(x_t|x_1, \dots, x_{t-1})$, where x_1, \dots, x_n are characters of SMILES representation of \mathbf{x} .

Alternatively, graph-based assembly strategies, either atom-based or fragment-based, can express molecules intuitively, and various studies have proposed using graph neural networks (GNN) to generate molecules (e.g., Nigam et al., 2019; Zhou et al., 2019; Jain et al., 2022). However, no GNN-based generative policy has shown superior performance over string-based generative policies from the observations in the PMO benchmark. Potentially, graph-based generating policies search for broader chemical space, including undesired ones (Gao et al., 2022a).

Another observation from the PMO benchmarks is that pre-training is inevitable since training the generative policy from scratch is excessively sample-inefficient. Therefore, our policy is pre-trained to maximize the likelihood of valid molecules on existing chemical datasets \mathcal{D}_{pre} , i.e.,

$$\mathcal{L}_{\text{pre}}(\mathbf{x}) = - \sum_{t=1}^n \log \pi_{\theta}(x_t | x_1, \dots, x_{t-1}). \quad (2)$$

Note that pre-training does not require oracle information.

3.2. GFlowNet Fine-tuning with Genetic Search

Next, we tune the generative policy through interactions with oracle functions so that the policy generates molecules with the more desired properties within the limited samples. To achieve this, we employ genetic search which iteratively improves the sampled solutions through GA operations. Then, the policy is trained to minimize the trajectory balance loss of GFlowNets with rank-based sampling.

Genetic search. To effectively search the higher-reward region, we employ a genetic algorithm that iteratively evolves populations through *crossover*, *mutation*, and *selection*. The proper design of genetic operations is widely recognized to impact optimization capability significantly. Therefore, we adopt the operations of the graph-based genetic algorithm, Graph GA (Jensen, 2019), which has proved its effectiveness in generating molecules with desired properties. The genetic search is performed as follows:

1. **Initialize a population \mathcal{D}_p :** Using rank-based sampling (see the following paragraph), the initial population is selected from the whole buffer \mathcal{D} , consisting of samples from the policy and previous genetic search.
2. **Generate offspring \mathcal{D}_o :** A child is generated from randomly chosen two parent molecules by combining the fragments (*crossover*). Then, the child is randomly modified (*mutation*).
3. **Select a new population \mathcal{D}'_p :** from $\mathcal{D}_p \cup \mathcal{D}_o$ using rank-based sampling (*selection*).
4. Set $\mathcal{D}_p \leftarrow \mathcal{D}'_p$ and go back to 2.

A detailed description is provided in Appendix B.

Rank-based Sampling. As a selection rule for the population in steps 1 and 3 in the genetic search, we utilize rank-based sampling (Tripp et al., 2020) to make the population is biased to the high-reward candidates. We samples molecules using the rank-based probability, i.e.,

$$\frac{(k|\mathcal{D}| + \text{rank}_{\mathcal{O}, \mathcal{D}}(\mathbf{x}))^{-1}}{\sum_{\mathbf{x} \in \mathcal{D}} (k|\mathcal{D}| + \text{rank}_{\mathcal{O}, \mathcal{D}}(\mathbf{x}))^{-1}}. \quad (3)$$

Here, k is a weight-shifting factor, and $\text{rank}_{\mathcal{O}, \mathcal{D}}(\mathbf{x})$ is a relative rank of value of $\mathcal{O}(\mathbf{x})$ in the dataset \mathcal{D} . Note that the next generation \mathcal{D}'_p is sampled from $\mathcal{D}_p \cup \mathcal{D}_o$ instead of \mathcal{D} in the population selection (step 3).

TB loss with KL penalty. By leveraging the off-policy property of GFlowNets (Bengio et al., 2021a), one of their notable advantages, the generative policy is trained using the trajectory balance loss in Equation (1). Additionally, we introduce an inverse temperature β , i.e., $\log R(\mathbf{x}) = -\beta \mathcal{O}(\mathbf{x})$, which makes us adjust desirable optimality capability and diversity. This study considers the generation of SMILES strings as an auto-regressive process, thus setting P_B to 1 for simplicity. It is worth mentioning that further enhancements can be achieved by learning P_B (Shen et al., 2023) by carefully considering the symmetric nature between SMILES string and graph isomorphism (Ma et al., 2023; Kim et al., 2023b).

Lastly, to ensure that the policy does not deviate excessively from the pre-trained policy, we introduce a KL penalty inspired by the works in language model fine-tuning, e.g., Ziegler et al. (2019) and Rafailov et al. (2023). Thus, our model is tuned to minimize the following loss function:

$$\mathcal{L} = \mathcal{L}_{\text{TB}}(\tau; \theta) + \alpha \text{KL}(\pi_{\theta}(x) || \pi_{\text{ref}}(x)), \quad (4)$$

where π_{ref} denotes the reference policy, i.e., the pre-trained policy. As a result, π_{θ} is trained to generate desired (by \mathcal{L}_{TB}) and valid (by π_{ref}) molecules.

4. Related Works

4.1. Genetic Algorithms

Genetic algorithm (GA) is a representative meta-heuristic inspired by the evolutionary process, encompassing a broad range of algorithms that operate in similar ways, rather than describing a specific algorithm. This subsection focuses on discussing the application of GA in molecular optimization. Additionally, various molecular assembly strategies beyond graph representations have been employed in GA. As one of the seminal works, Jensen (2019) presented Graph GA, where operations are defined on 2-dimensional molecular graphs. Note that our method also adopts operations of Graph GA in the genetic search. Various strategies for molecular assembly, not limited to graphs, have been utilized in GA (Yoshikawa et al., 2018; Nigam et al., 2021; Gao et al., 2022b).

A recent contribution by Tripp & Hernández-Lobato (2023) introduces an enhanced version of Graph GA with a more careful selection of hyperparameters. They introduce quantile-uniform sampling to bias the population towards containing higher reward samples while maintaining diversity. Experimental results from Mol GA demonstrate the

effectiveness of GAs as strong baselines, achieving state-of-the-art (SOTA) performance in the PMO benchmark.

Another notable work is a genetic expert-guided learning (GEGL; Ahn et al., 2020), which shares the concept of guiding a neural network policy through GA. In GEGL, the policy is trained with the GA-based expert policy using imitation learning, which is the main difference from ours. In addition, GEGL utilizes genetic search without evolving generations, specifically conducting steps 1 and 2 only. Since the samples that the policy imitates need to be selective, the priority queue needs to keep samples selectively. Thus, a substantial number of samples are screened, i.e., evaluated but not used. While GEGL demonstrates competitive performance, it necessitates a relatively high number of samples, as detailed in the results in Section 5.3.

4.2. GFlowNets

Generative flow networks (GFlowNets or GFN; Bengio et al., 2021b) have drawn significant attention in the field of biomolecular design, such as molecular optimization and biological sequence design (Bengio et al., 2021a; Jain et al., 2022; Shen et al., 2023; Kim et al., 2023d). Bengio et al. (2021a) proposed GFlowNet with flow matching loss, a temporal difference-like loss, and generate molecular graphs. Based on this work, Jain et al. (2022) suggested the model-based GFlowNet, called GFlowNet-AL. GFlowNet-AL substantially generates diverse and novel batches in several biological sequence design tasks. These two works are also investigated and show relatively low sample efficiency Gao et al. (2022a). To mitigate a low-reward exploration tendency of GFlowNets, Shen et al. (2023) suggested the prioritized replay training of high-reward and the guided trajectory balance objective. They effectively improve the sample efficiency on biochemical design tasks by addressing a credit assignment problem. Recently, the concept of integrating search algorithms to encourage exploration is also present in the work of Kim et al. (2023d), local search GFlowNets (LS-GFN), where they use backward policy to backtrack the trajectory and reconstruct it using forward policy partially. The effectiveness of such methods is contingent upon their exploratory capabilities of backward policy (Kim et al., 2023d). Direct application to auto-regressive policies (e.g., SMILES generation), characterized by a singular backtracking path, is thus unsuitable.

In addition to these developments, various studies have sought to enhance GFlowNets through new training losses (Malkin et al., 2022; Madan et al., 2023), credit assignment methods (Pan et al., 2023; Jang et al., 2023), and improved exploration techniques (Pan et al., 2022; Rector-Brooks et al., 2023; Kim et al., 2023c). Our contribution lies in proposing an efficient exploration method that leverages genetic algorithms, further enriching the landscape of

GFlowNet advancements.

5. Experiments

5.1. Implementation of Genetic GFN

Pre-training. As we employ the same policy as REINVENT, pre-training is conducted, following Gao et al. (2022a), using the ZINC 250K dataset (Sterling & Irwin, 2015) to maximize log-likelihoods for molecules within the dataset, facilitating the ability to generate valid molecules. More details about pre-training are provided in Appendix A.2. For fair comparisons with REINVENT, we consistently use the same pre-trained model to REINVENT and Genetic GFN across all experiments.

Hyperparameter setup. The KL penalty coefficient α is configured at 0.001. On the other hand, the inverse temperature β and weight-shifting factor k can be flexibly assigned to adjust the trade-off between achieving high scores and promoting diversity; refer to Section 5.4 for details. We adopt the setup of REINVENT related to the model, e.g., batch size and learning rate. For genetic search parameters, we set the mutation rate as 0.01, consistent with GEGL, and the population size as 64, the same as the batch size. The offspring size and the GA generation are determined as 8 and 2 through hyperparameter searching.

5.2. Experiments in PMO Benchmark

This subsection provides the experimental results in PMO benchmark setup. All methods are evaluated using various pharmaceutically-relevant oracles with 10,000 calls.

Metric. The area under the curve (AUC) of Top- K samples is employed as a primary performance metric. In contrast to the average score of Top- K , AUC also considers sample efficiency, not only the optimality ability. Mainly, $K = 10$ is used since de novo molecular optimization aims to find candidate molecules to proceed to the later stage of development. AUC values are computed every 100 oracle calls, and the reported values are normalized within the range of 0 to 1. When we compute the ranks of each method, the average score of Top- K , where K is 1, 10, and 100, is also measured.

PMO Baselines. We employ Top-8 methods from the PMO benchmark since they recorded the best AUC Top-10 in at least one oracle. The baseline methods include various ranges of algorithms and representation strategies. Firstly, REINVENT (Olivecrona et al., 2017) is an RL method that tunes the policy with adjusted likelihood. We denote

Genetic-guided GFlowNets

Table 1. Mean and standard deviation of AUC Top-10 from five independent runs with different seeds. Top-8 methods in the PMO benchmark and Mol GA are employed as baselines.

Oracle	Genetic GFN (Ours)	Mol GA	SMILES REINVENT	GP BO	SELFIES REINVENT
albuterol_similarity	0.949 ± 0.010	0.928 ± 0.015	0.881 ± 0.016	0.902 ± 0.011	0.867 ± 0.025
amlodipine_mpo	0.761 ± 0.019	0.740 ± 0.055	0.644 ± 0.019	0.579 ± 0.035	0.621 ± 0.015
celecoxib_rediscovery	0.802 ± 0.029	0.629 ± 0.062	0.717 ± 0.027	0.746 ± 0.025	0.588 ± 0.062
deco_hop	0.733 ± 0.109	0.656 ± 0.013	0.662 ± 0.044	0.615 ± 0.009	0.638 ± 0.016
drd2	0.974 ± 0.006	0.950 ± 0.004	0.957 ± 0.007	0.941 ± 0.017	0.953 ± 0.009
fexofenadine_mpo	0.856 ± 0.039	0.835 ± 0.012	0.781 ± 0.013	0.726 ± 0.004	0.740 ± 0.012
gsk3b	0.881 ± 0.042	0.894 ± 0.025	0.885 ± 0.031	0.861 ± 0.027	0.821 ± 0.041
isomers_c7h8n2o2	0.969 ± 0.003	0.926 ± 0.014	0.942 ± 0.012	0.883 ± 0.040	0.873 ± 0.041
isomers_c9h10n2o2pf2cl	0.897 ± 0.007	0.894 ± 0.005	0.838 ± 0.030	0.805 ± 0.007	0.844 ± 0.016
jnk3	0.764 ± 0.069	0.835 ± 0.040	0.782 ± 0.029	0.611 ± 0.080	0.624 ± 0.048
median1	0.379 ± 0.010	0.329 ± 0.006	0.363 ± 0.011	0.298 ± 0.016	0.353 ± 0.006
median2	0.294 ± 0.007	0.284 ± 0.035	0.281 ± 0.002	0.296 ± 0.011	0.252 ± 0.010
mestranol_similarity	0.708 ± 0.057	0.762 ± 0.048	0.634 ± 0.042	0.631 ± 0.093	0.589 ± 0.040
osimertinib_mpo	0.860 ± 0.008	0.853 ± 0.005	0.834 ± 0.010	0.788 ± 0.005	0.819 ± 0.005
perindopril_mpo	0.595 ± 0.014	0.610 ± 0.038	0.535 ± 0.015	0.494 ± 0.006	0.533 ± 0.024
qed	0.942 ± 0.000	0.941 ± 0.001	0.941 ± 0.000	0.937 ± 0.002	0.940 ± 0.000
ranolazine_mpo	0.819 ± 0.018	0.830 ± 0.010	0.770 ± 0.005	0.741 ± 0.010	0.736 ± 0.008
scaffold_hop	0.615 ± 0.100	0.568 ± 0.017	0.551 ± 0.024	0.535 ± 0.007	0.521 ± 0.014
sitagliptin_mpo	0.634 ± 0.039	0.677 ± 0.055	0.470 ± 0.041	0.461 ± 0.057	0.492 ± 0.055
thiothixene_rediscovery	0.583 ± 0.034	0.544 ± 0.067	0.544 ± 0.026	0.544 ± 0.038	0.497 ± 0.043
trogliatzone_rediscovery	0.511 ± 0.054	0.487 ± 0.024	0.458 ± 0.018	0.404 ± 0.025	0.342 ± 0.022
valsartan_smarts	0.135 ± 0.271	0.000 ± 0.000	0.182 ± 0.363	0.000 ± 0.000	0.000 ± 0.000
zaleplon_mpo	0.552 ± 0.033	0.514 ± 0.033	0.533 ± 0.009	0.466 ± 0.025	0.509 ± 0.009
Sum	16.213	15.686	15.185	14.264	14.152
Old Rank	N/A	N/A	1	4	3
New Rank	1	2	3	4	5
Diversity	0.432	0.465	0.468	0.617	0.555

Oracle	Graph GA	SMILES LSTM-HC	STONED	SynNet	SMILE GA
albuterol_similarity	0.859 ± 0.013	0.731 ± 0.008	0.765 ± 0.048	0.568 ± 0.033	0.649 ± 0.079
amlodipine_mpo	0.657 ± 0.022	0.598 ± 0.021	0.608 ± 0.020	0.566 ± 0.006	0.520 ± 0.017
celecoxib_rediscovery	0.593 ± 0.092	0.552 ± 0.014	0.378 ± 0.043	0.439 ± 0.035	0.361 ± 0.038
deco_hop	0.602 ± 0.012	0.837 ± 0.018	0.612 ± 0.007	0.635 ± 0.043	0.612 ± 0.005
drd2	0.973 ± 0.001	0.941 ± 0.005	0.935 ± 0.014	0.970 ± 0.006	0.958 ± 0.015
fexofenadine_mpo	0.762 ± 0.014	0.733 ± 0.002	0.791 ± 0.014	0.750 ± 0.016	0.705 ± 0.025
gsk3b	0.817 ± 0.057	0.846 ± 0.019	0.666 ± 0.022	0.713 ± 0.057	0.714 ± 0.038
isomers_c7h8n2o2	0.949 ± 0.020	0.830 ± 0.019	0.930 ± 0.012	0.862 ± 0.004	0.821 ± 0.070
isomers_c9h10n2o2pf2cl	0.839 ± 0.042	0.693 ± 0.018	0.897 ± 0.032	0.657 ± 0.030	0.853 ± 0.049
jnk3	0.652 ± 0.106	0.670 ± 0.014	0.509 ± 0.065	0.574 ± 0.103	0.353 ± 0.061
median1	0.285 ± 0.012	0.263 ± 0.007	0.264 ± 0.032	0.236 ± 0.015	0.187 ± 0.029
median2	0.255 ± 0.019	0.249 ± 0.003	0.254 ± 0.024	0.241 ± 0.007	0.178 ± 0.009
mestranol_similarity	0.571 ± 0.036	0.553 ± 0.040	0.620 ± 0.098	0.402 ± 0.017	0.419 ± 0.028
osimertinib_mpo	0.813 ± 0.006	0.801 ± 0.002	0.829 ± 0.012	0.793 ± 0.008	0.820 ± 0.021
perindopril_mpo	0.514 ± 0.025	0.491 ± 0.006	0.484 ± 0.016	0.541 ± 0.021	0.442 ± 0.016
qed	0.937 ± 0.001	0.939 ± 0.001	0.942 ± 0.000	0.941 ± 0.001	0.941 ± 0.002
ranolazine_mpo	0.718 ± 0.017	0.728 ± 0.005	0.764 ± 0.023	0.749 ± 0.009	0.723 ± 0.023
scaffold_hop	0.513 ± 0.026	0.529 ± 0.004	0.515 ± 0.025	0.506 ± 0.012	0.507 ± 0.008
sitagliptin_mpo	0.498 ± 0.048	0.309 ± 0.015	0.600 ± 0.103	0.297 ± 0.033	0.449 ± 0.068
thiothixene_rediscovery	0.483 ± 0.034	0.440 ± 0.014	0.375 ± 0.029	0.397 ± 0.012	0.310 ± 0.019
trogliatzone_rediscovery	0.373 ± 0.013	0.369 ± 0.015	0.309 ± 0.030	0.280 ± 0.006	0.262 ± 0.019
valsartan_smarts	0.000 ± 0.000	0.011 ± 0.021	0.000 ± 0.000	0.000 ± 0.000	0.000 ± 0.000
zaleplon_mpo	0.468 ± 0.025	0.470 ± 0.004	0.484 ± 0.015	0.493 ± 0.014	0.470 ± 0.029
Sum	14.131	13.583	13.531	12.610	12.254
Old Rank	2	6	5	8	7
New Rank	6	7	8	9	10
Diversity	0.661	0.686	0.498	0.728	0.596

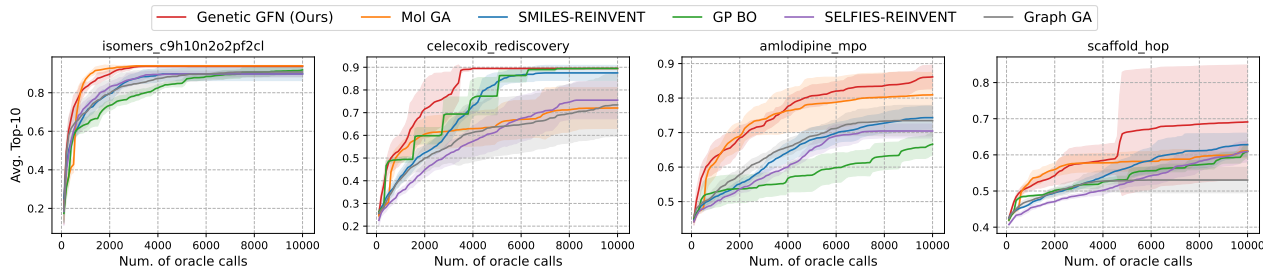


Figure 3. The optimization curve of the average scores of Top-10 over the oracle calls.

SMILES-REINVENT and SELFIES-REINVENT¹ according to which string representations are employed. Graph GA (Jensen, 2019), STONED (Nigam et al., 2021), SMILES GA (Brown et al., 2019), and SynNet (Gao et al., 2022b) are genetic algorithms that utilize different assembly strategies; they use fragment-based graphs, SELFIES, SMILES, and synthesis, respectively. Additionally, we adopt the hill climbing method, SMILES-LSTM-HC (Brown et al., 2019), and Bayesian optimization, GP BO (Tripp et al., 2021). SMILES-LSTM-HC iteratively generates samples and fine-tunes the policy with high-reward samples, especially using imitation learning. On the other hand, GP BO builds a surrogate model with the Gaussian process (GP) and optimizes the GP acquisition functions with Graph GA in the inner loop. Moreover, we adopt an additional method, Mol GA (Tripp & Hernández-Lobato, 2023), which is an advanced version of Graph GA and outperforms other baselines.

Hyperparameter setup. We follow the provided hyperparameter setup of baseline methods originally implemented in the PMO benchmark. For Mol GA, we adopt the original implementation,² and according to the paper, the offspring size is set to five. Additionally, population sizes are searched following the PMO guidelines; see Appendix C.

Other setting. We use the later version of oracle library, TDC 0.4.0, whereas the results in Gao et al. (2022a) are reported with TDC 0.3.6. In addition, we introduce an additional early stopping criteria, which terminates the process when the policy cannot generate new molecules within predefined steps. The results are reported with independent runs using five random seeds ([0, 1, 2, 3, 4]).

Results. The main results are presented in Table 1; more results are provided in Appendix D. Moreover, Figure 3 visually presents the Top-10 average across the computational budget, i.e., the number of oracle calls, providing a concise overview of the results. As shown in Table 1, Genetic GFN outperforms the other baselines with a total of 16.213 and

¹SELFReferencIng Embedded Strings (SELFIES; Krenn et al., 2020) is a string-based representation

²Available at https://github.com/AustinT/mol_ga

Table 2. The mean of AUC Top-10 from five independent runs.

Oracle	Genetic GFN			GEGl
	Ours	w/o GS	w/o KL	
albuterol_similarity	0.949	0.942	0.946	0.842
amlodipine_mpo	0.761	0.686	0.705	0.626
celecoxib_rediscovery	0.802	0.804	0.810	0.699
deco_hop	0.733	0.746	0.664	0.656
drd2	0.974	0.962	0.975	0.898
fexofenadine_mpo	0.856	0.818	0.822	0.769
gsk3b	0.881	0.889	0.892	0.816
isomers_c7h8n2o2	0.969	0.939	0.969	0.930
isomers_c9h10n2o2pf2cl	0.897	0.884	0.881	0.808
jnk3	0.764	0.799	0.627	0.580
median1	0.379	0.369	0.367	0.338
median2	0.294	0.284	0.296	0.274
mestranol_similarity	0.708	0.666	0.695	0.599
osimertinib_mpo	0.860	0.854	0.851	0.832
perindopril_mpo	0.595	0.560	0.610	0.537
qed	0.942	0.942	0.942	0.941
ranolazine_mpo	0.819	0.808	0.818	0.730
scaffold_hop	0.615	0.608	0.583	0.531
sitagliptin_mpo	0.634	0.509	0.644	0.402
thiothixene_rediscovery	0.583	0.576	0.605	0.515
troglitazone_rediscovery	0.511	0.540	0.517	0.420
valsartan_smarts	0.135	0.000	0.166	0.119
zaleplon_mpo	0.552	0.551	0.543	0.492
Sum	16.213	15.736	15.928	14.354

attains the highest AUC Top-10 values in 14 out of 23 oracle functions. It is noteworthy that the reported scores are higher than the original results overall, and there are some alterations in the ranks, e.g., GP BO and Graph GA. As explained, variations in TDC versions and random seeds might account for these differences. The results of diversity and SA score for each oracle are presented in Appendix D.

5.3. Ablation Studies

In this subsection, we assess the efficacy of Genetic GFN by conducting ablation studies on its main components of oracle-directed fine-tuning: genetic search, KL penalty, and GFlowNet training. As detailed in Section 4.1, we compare with GEGl, an ablated version of our approach that utilizes imitation learning with a reward-priority queue instead of GFlowNet training with rank-based sampling.

Table 3. The score-diversity trade-off with different β .

Oracle	$\beta = 5$	$\beta = 10$	$\beta = 30$	$\beta = 50$
AUC Top-1	15.247	15.385	16.248	16.527
AUC Top-10	14.597	14.735	15.815	16.213
AUC Top-100	13.116	13.348	14.943	15.516
Diversity	0.670	0.663	0.528	0.432

Implementation and hyperparameters. As GEGL is not included in the benchmark, we incorporated the original implementation of GEGL³ into the PMO benchmark framework. We basically follow the original setup, such as mutation rate. Yet, we have searched for the number of samples for each policy and the sizes of the priority queue, which significantly impact performance. Additional details are provided in Appendix C.

Results. As shown in Table 2, each component of ours, genetic search, KL penalty, and TB loss with rank-based sampling, significantly contribute to performance improvement. Due of the lack of space, standard deviations are omitted; we provide the full results in Appendix D. Notably, the results of Genetic GFN without genetic search (denoted as ‘w/o GS’) and without the KL penalty (denoted as ‘w/o KL’) also outperform all baselines in the PMO benchmark. Moreover, although GEGL shows relatively sample-inefficient results compared to ours, it attains a superior score compared to GP BO, which holds the 4th rank in the PMO benchmark.

5.4. Trade-off Between Scores and Diversity

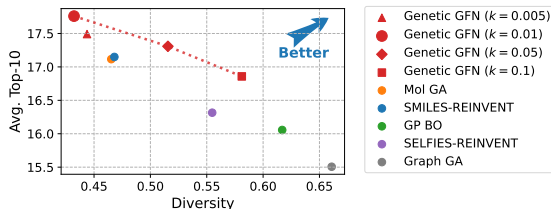
As mentioned in Section 5.1, we present experimental results to demonstrate the controllability of the score-diversity trade-off through adjustments in the inverse temperature β . Decreasing the inverse temperature gives more diverse candidates. The results in Figure 1 and Table 3 demonstrate adjustments of β can control the trade-off between score and diversity, achieving Pareto-curve to other baselines in the benchmark. Notably, Genetic GFN with $\beta = 30$ gives higher AUC Top-10 with a greater diversity compared to the SOTA GA method (Mol GA: 15.686 with a diversity of 0.465) and RL method (REINVENT: 15.185 with a diversity of 0.468). It is worth emphasizing that our method produces a Pareto curve, as illustrated in Figure 1 in Section 1.

Similarly, the weight-shift factor k in rank-based sampling affects the score-diversity trade-off. As depicted in Table 4, increasing k gives more diverse candidates, like decreasing β . Yet, we recommend adjusting the inverse temperature parameter β rather than k .

³Available at <https://github.com/sungsoo-ahn/genetic-expert-guided-learning/tree/main>.

Table 4. The score-diversity trade-off by varying k with fixed β .

Oracle	$k = 0.1$	$k = 0.05$	$k = 0.01$	$k = 0.005$
AUC Top-1	15.246	15.801	16.527	16.323
AUC Top-10	14.652	15.330	16.213	16.040
AUC Top-100	13.597	14.453	15.516	15.418
Diversity	0.581	0.515	0.432	0.444

Figure 4. The average score and diversity with adjustments of k .

5.5. Additional Analysis

Compared to graph-based GFlowNets. We compare our method with graph-based GFlowNets in the PMO benchmark. GFlowNets directly construct molecular graphs and consider the symmetries of the graph generation. The experimental results show that our method successfully enhances sample efficiency in terms of discovering molecules with desired properties. In comparison, GFlowNet and GFlowNet-AL generate considerably diverse molecules, which is one of the primary goals; please refer to Appendix D.3.

Genetic GFN with SELFIES representation. Genetic GFN with SELFIES generation achieves the improved sample efficiency, 14.986 overall, outperforming 19 out of 23 oracles compared to SELFIES-REINVENT; see Appendix D.

Sensitivity analysis. We provide the experimental results by varying the hyperparameters, such as the offspring size and the number of training loops; see Appendix D.6.

6. Discussion

This paper proposes a Genetic-guided GFlowNet (Genetic GFN), which substantially improves sample efficiency, i.e., the higher score within the limited number of reward evaluations, by effectively handling the trade-off between score-diversity. Noticeably, our method shows steerability for the score-diversity trade-off by adjusting the inverse temperature during the GFlowNet fine-tuning phase. The proposed method adopts an unsupervised pre-training and fine-tuning framework, wherein GFlowNet training is guided by the sophisticated search algorithm, i.e., the genetic algorithm. We believe that our algorithmic discovery extends beyond the realm of de novo molecule optimization. We discuss connecting two emerging areas.

Fine-tuning Large Language Model. An intriguing application lies in the context of large language models (LLMs), which share similar algorithmic structures, such as unsupervised learning and sample-efficient fine-tuning. Current fine-tuning methods for LLMs, relying on human preferences (Ziegler et al., 2019; Rafailov et al., 2023), may necessitate additional online human feedback to better align with human preferences, highlighting the importance of *sample-efficient* fine-tuning.

Furthermore, recent advancements in GFlowNets applied to LLMs (Hu et al., 2023), including preference optimization (Li et al., 2023), have emphasized the need for *diversity* in the fine-tuning process. Therefore, balancing the trade-off between *sample efficiency* and *diversity* can emerge as a crucial new challenge for LLMs. In this context, our method can serve as a valuable precedent.

Neural combinatorial optimization. Our algorithm exhibits similarities with recent developments in neural combinatorial optimization (Bello et al., 2016; Kool et al., 2018), a field that utilizes deep neural networks to amortize the search process in combinatorial optimization. One of the approaches in this area has addressed problems like the traveling salesman and the capacitated vehicle routing problem (CVRP) through a constructive policy (Kwon et al., 2020; Kim et al., 2021; 2022) which sequentially adds elements (action) into partial solution (state) to complete solution. Some works also focused on enhancing training and sample efficiency of constructive policy (Hottung et al., 2021; Son et al., 2023; Kim et al., 2023a).

The methodology of generating combinatorial solutions via a constructive policy mirrors our technique for the sequential generation of molecules. Moreover, our method is compatible with advanced strategies like the hybrid genetic search (HGS; Vidal et al., 2012), which is acknowledged for its effectiveness in solving CVRP. As a potential direction for future work, one can explore the integration of HGS for genetic search processes and GFlowNets for constructing solutions to the Capacitated Vehicle Routing Problem (CVRP).

References

- Ahn, S., Kim, J., Lee, H., and Shin, J. Guiding deep molecular optimization with genetic exploration. *Advances in neural information processing systems*, 33:12008–12021, 2020.
- Bello, I., Pham, H., Le, Q. V., Norouzi, M., and Bengio, S. Neural combinatorial optimization with reinforcement learning. *arXiv preprint arXiv:1611.09940*, 2016.
- Bengio, E., Jain, M., Korablyov, M., Precup, D., and Bengio, Y. Flow network based generative models for non-iterative diverse candidate generation. *Advances in Neural Information Processing Systems*, 34:27381–27394, 2021a.
- Bengio, Y., Lahlou, S., Deleu, T., Hu, E. J., Tiwari, M., and Bengio, E. Gflownet foundations. *arXiv preprint arXiv:2111.09266*, 2021b.
- Bickerton, G. R., Paolini, G. V., Besnard, J., Muresan, S., and Hopkins, A. L. Quantifying the chemical beauty of drugs. *Nature chemistry*, 4(2):90–98, 2012.
- Brown, N., Fiscato, M., Segler, M. H., and Vaucher, A. C. GuacaMol: benchmarking models for de novo molecular design. *Journal of chemical information and modeling*, 59(3):1096–1108, 2019.
- Chung, J., Gulcehre, C., Cho, K., and Bengio, Y. Empirical evaluation of gated recurrent neural networks on sequence modeling. *arXiv preprint arXiv:1412.3555*, 2014.
- Gao, W., Fu, T., Sun, J., and Coley, C. Sample efficiency matters: a benchmark for practical molecular optimization. *Advances in Neural Information Processing Systems*, 35:21342–21357, 2022a.
- Gao, W., Mercado, R., and Coley, C. W. Amortized tree generation for bottom-up synthesis planning and synthesizable molecular design. In *International Conference on Learning Representations*, 2022b. URL <https://openreview.net/forum?id=FRxhHdnxt1>.
- Gómez-Bombarelli, R., Wei, J. N., Duvenaud, D., Hernández-Lobato, J. M., Sánchez-Lengeling, B., Sheberla, D., Aguilera-Iparraguirre, J., Hirzel, T. D., Adams, R. P., and Aspuru-Guzik, A. Automatic chemical design using a data-driven continuous representation of molecules. *ACS central science*, 4(2):268–276, 2018.
- Hottung, A., Kwon, Y.-D., and Tierney, K. Efficient active search for combinatorial optimization problems. *arXiv preprint arXiv:2106.05126*, 2021.
- Hu, E. J., Jain, M., Elmoznino, E., Kaddar, Y., Lajoie, G., Bengio, Y., and Malkin, N. Amortizing intractable inference in large language models, 2023.
- Huang, K., Fu, T., Gao, W., Zhao, Y., Roohani, Y. H., Leskovec, J., Coley, C. W., Xiao, C., Sun, J., and Zitnik, M. Therapeutics data commons: Machine learning datasets and tasks for drug discovery and development. In *Thirty-fifth Conference on Neural Information Processing Systems Datasets and Benchmarks Track (Round 1)*, 2021. URL <https://openreview.net/forum?id=8nvgnORnoWr>.
- Hughes, J. P., Rees, S., Kalindjian, S. B., and Philpott, K. L. Principles of early drug discovery. *British journal of pharmacology*, 162(6):1239–1249, 2011.

- Jain, M., Bengio, E., Hernandez-Garcia, A., Rector-Brooks, J., Dossou, B. F., Ekbote, C. A., Fu, J., Zhang, T., Kilgour, M., Zhang, D., et al. Biological sequence design with gflownets. In *International Conference on Machine Learning*, pp. 9786–9801. PMLR, 2022.
- Jang, H., Kim, M., and Ahn, S. Learning energy decompositions for partial inference of gflownets, 2023.
- Jensen, J. H. A graph-based genetic algorithm and generative model/monte carlo tree search for the exploration of chemical space. *Chemical science*, 10(12):3567–3572, 2019.
- Kim, H., Kim, M., Ahn, S., and Park, J. Enhancing sample efficiency in black-box combinatorial optimization via symmetric replay training, 2023a.
- Kim, H., Kim, M., Ahn, S., and Park, J. Symmetric Replay Training: Enhancing sample efficiency in deep reinforcement learning for combinatorial optimization, 2023b.
- Kim, M., Park, J., et al. Learning collaborative policies to solve np-hard routing problems. *Advances in Neural Information Processing Systems*, 34:10418–10430, 2021.
- Kim, M., Park, J., and Park, J. Sym-nco: Leveraging symmetricity for neural combinatorial optimization. *Advances in Neural Information Processing Systems*, 35:1936–1949, 2022.
- Kim, M., Ko, J., Zhang, D., Pan, L., Yun, T., Kim, W., Park, J., and Bengio, Y. Learning to scale logits for temperature-conditional GFlowNets. *arXiv preprint arXiv:2310.02823*, 2023c.
- Kim, M., Yun, T., Bengio, E., Zhang, D., Bengio, Y., Ahn, S., and Park, J. Local search gflownets. *arXiv preprint arXiv:2310.02710*, 2023d.
- Kool, W., van Hoof, H., and Welling, M. Attention, learn to solve routing problems! In *International Conference on Learning Representations*, 2018.
- Krenn, M., Häse, F., Nigam, A., Friederich, P., and Aspuru-Guzik, A. Self-referencing embedded strings (SELFIES): A 100% robust molecular string representation. *Machine Learning: Science and Technology*, 1(4):045024, 2020.
- Kwon, Y.-D., Choo, J., Kim, B., Yoon, I., Gwon, Y., and Min, S. POMO: Policy optimization with multiple optima for reinforcement learning. *Advances in Neural Information Processing Systems*, 33:21188–21198, 2020.
- Li, Y., Zhang, L., and Liu, Z. Multi-objective de novo drug design with conditional graph generative model. *Journal of cheminformatics*, 10:1–24, 2018.
- Li, Y., Luo, S., Shao, Y., and Hao, J. Gflownets with human feedback, 2023.
- Ma, G., Bengio, E., Bengio, Y., and Zhang, D. Baking symmetry into gflownets. In *NeurIPS 2023 AI for Science Workshop*, 2023.
- Madan, K., Rector-Brooks, J., Korablyov, M., Bengio, E., Jain, M., Nica, A. C., Bosc, T., Bengio, Y., and Malkin, N. Learning gflownets from partial episodes for improved convergence and stability. In *International Conference on Machine Learning*, pp. 23467–23483. PMLR, 2023.
- Malkin, N., Jain, M., Bengio, E., Sun, C., and Bengio, Y. Trajectory balance: Improved credit assignment in gflownets. *Advances in Neural Information Processing Systems*, 35:5955–5967, 2022.
- Nigam, A., Friederich, P., Krenn, M., and Aspuru-Guzik, A. Augmenting genetic algorithms with deep neural networks for exploring the chemical space. In *International Conference on Learning Representations*, 2019.
- Nigam, A., Pollice, R., Krenn, M., dos Passos Gomes, G., and Aspuru-Guzik, A. Beyond generative models: superfast traversal, optimization, novelty, exploration and discovery (STONED) algorithm for molecules using SELFIES. *Chemical science*, 12(20):7079–7090, 2021.
- Olivecrona, M., Blaschke, T., Engkvist, O., and Chen, H. Molecular de-novo design through deep reinforcement learning. *Journal of cheminformatics*, 9(1):1–14, 2017.
- Pan, L., Zhang, D., Courville, A., Huang, L., and Bengio, Y. Generative augmented flow networks. In *The Eleventh International Conference on Learning Representations*, 2022.
- Pan, L., Malkin, N., Zhang, D., and Bengio, Y. Better training of gflownets with local credit and incomplete trajectories. *arXiv preprint arXiv:2302.01687*, 2023.
- Polishchuk, P. CReM: chemically reasonable mutations framework for structure generation. *Journal of Cheminformatics*, 12(1):1–18, 2020.
- Rafailov, R., Sharma, A., Mitchell, E., Ermon, S., Manning, C. D., and Finn, C. Direct preference optimization: Your language model is secretly a reward model. *arXiv preprint arXiv:2305.18290*, 2023.
- Rector-Brooks, J., Madan, K., Jain, M., Korablyov, M., Liu, C.-H., Chandar, S., Malkin, N., and Bengio, Y. Thompson sampling for improved exploration in gflownets. *arXiv preprint arXiv:2306.17693*, 2023.
- Shen, M. W., Bengio, E., Hajiramezanali, E., Loukas, A., Cho, K., and Biancalani, T. Towards understanding and

- improving GFlowNet training. In *Proceedings of the 40th International Conference on Machine Learning*, 2023.
- Son, J., Kim, M., Kim, H., and Park, J. Meta-SAGE: Scale meta-learning scheduled adaptation with guided exploration for mitigating scale shift on combinatorial optimization. In Krause, A., Brunskill, E., Cho, K., Engelhardt, B., Sabato, S., and Scarlett, J. (eds.), *Proceedings of the 40th International Conference on Machine Learning*, volume 202 of *Proceedings of Machine Learning Research*, pp. 32194–32210. PMLR, 23–29 Jul 2023. URL <https://proceedings.mlr.press/v202/son23a.html>.
- Sterling, T. and Irwin, J. J. Zinc 15–ligand discovery for everyone. *Journal of chemical information and modeling*, 55(11):2324–2337, 2015.
- Tripp, A. and Hernández-Lobato, J. M. Genetic algorithms are strong baselines for molecule generation. *arXiv preprint arXiv:2310.09267*, 2023.
- Tripp, A., Daxberger, E., and Hernández-Lobato, J. M. Sample-efficient optimization in the latent space of deep generative models via weighted retraining. *Advances in Neural Information Processing Systems*, 33:11259–11272, 2020.
- Tripp, A., Simm, G. N., and Hernández-Lobato, J. M. A fresh look at de novo molecular design benchmarks. In *NeurIPS 2021 AI for Science Workshop*, 2021.
- Vidal, T., Crainic, T. G., Gendreau, M., Lahrichi, N., and Rei, W. A hybrid genetic algorithm for multidepot and periodic vehicle routing problems. *Operations Research*, 60(3):611–624, 2012.
- Weininger, D. SMILES, a chemical language and information system. 1. introduction to methodology and encoding rules. *Journal of chemical information and computer sciences*, 28(1):31–36, 1988.
- Yan, C., Barlow, S., Wang, Z., Yan, H., Jen, A. K.-Y., Marder, S. R., and Zhan, X. Non-fullerene acceptors for organic solar cells. *Nature Reviews Materials*, 3(3): 1–19, 2018.
- Yoshikawa, N., Terayama, K., Sumita, M., Homma, T., Oono, K., and Tsuda, K. Population-based de novo molecule generation, using grammatical evolution. *Chemistry Letters*, 47(11):1431–1434, 2018.
- Zhou, Z., Kearnes, S., Li, L., Zare, R. N., and Riley, P. Optimization of molecules via deep reinforcement learning. *Scientific reports*, 9(1):1–10, 2019.
- Ziegler, D. M., Stiennon, N., Wu, J., Brown, T. B., Radford, A., Amodei, D., Christiano, P., and Irving, G. Fine-tuning language models from human preferences. *arXiv preprint arXiv:1909.08593*, 2019.
- Zimmermann, H., Lindsten, F., van de Meent, J.-W., and Naesseth, C. A. A variational perspective on generative flow networks. *Transactions on Machine Learning Research*, 2023. ISSN 2835-8856. URL <https://openreview.net/forum?id=AZ4GobeSLq>.

A. Implementation Details of Genetic GFN

A.1. Pseudo-code

Algorithm 1 Fine-tuning with Genetic GFN

```

1: Set  $\pi_\theta \leftarrow \pi_{\text{pre}}, \mathcal{D} \leftarrow \emptyset$ 
2: while  $|\mathcal{D}| \leq \text{numOracle}$  do
3:    $\triangleright$  SAMPLE CANDIDATES
4:    $x \sim \pi_\theta(\cdot)$ 
5:   Update  $\mathcal{D} \leftarrow \mathcal{D} \cup \{x, \mathcal{O}(x)\}$ 
6:    $\triangleright$  GENETIC SEARCH
7:   Initialize population  $\mathcal{D}_p$  from  $\mathcal{D}$  with rank-based sampling
8:   for  $n = 1$  to numGen do
9:     while  $|\mathcal{D}_o| \leq \text{numOff}$  do
10:       $x \leftarrow \text{Crossover}(x_1, x_2)$ , for  $x_1, x_2 \in \mathcal{D}_p$ 
11:       $x' \leftarrow \text{Mutate}(x)$ 
12:      if  $x'$  is valid then
13:         $\mathcal{D} \leftarrow \mathcal{D} \cup \{x', \mathcal{O}(x')\}$ 
14:         $\mathcal{D}_o \leftarrow \mathcal{D}_o \cup \{x', \mathcal{O}(x')\}$ 
15:      end if
16:    end while
17:    Update  $\mathcal{D}_p$  from  $\mathcal{D}_p \cup \mathcal{D}_o$  with rank-based sampling
18:  end for
19:   $\triangleright$  GFLOWNET TRAINING
20:  for  $k = 1$  to numTrain do
21:    Get  $\mathcal{B}$  from  $\mathcal{D}$  with rank-based sampling
22:    Minimize  $\frac{1}{|\mathcal{B}|} \sum_{x \in \mathcal{B}} \mathcal{L}_{\text{TB}} + \alpha \text{KL}(\pi_\theta(x) || \pi_{\text{pre}}(x))$ 
23:  end for
24: end while

```

A.2. Network Architecture and Pre-training

Network architecture. Our policy network is parameterized using a recurrent neural network containing multiple GRU cells (Chung et al., 2014). In molecular optimization, RNN-based models with string molecular representations have proven to be successful (e.g., Olivecrona et al., 2017; Ahn et al., 2020). In experiments, we employ the same hyperparameters to directly compare with REINVENT, whose input embedding dimension is 128, and hidden dimension is 512 with three layers.

Pre-training. According to the PMO benchmark guidelines (Gao et al., 2022a), the pre-training is conducted on ZINC 250K. Since the network architecture is the same as REINVENT, we use the pre-trained model in the experiments. It allows the direct comparison of fine-tuning approaches.

B. Genetic Operations

This section provides details for each operation in our genetic search. Note that we adopt Graph GA of Jensen (2019), which has demonstrated its powerful performances and has been adopted by GA-related works like Mol GA (Tripp & Hernández-Lobato, 2023) and GEGL (Ahn et al., 2020). Please refer to the original work of Jensen (2019) for further details.

B.1. Crossover

A crossover operation is conducted to generate a new candidate (called offspring) by exchanging the genetic information of a pair of selected individuals (parents). This process mimics the crossover of genetic material in biological reproduction. In the context of molecular optimization with graphs, the crossover operation is conducted in two types: ‘ring crossover’ and ‘non-ring crossover with a 50% probability.

These two main crossover operations perform crossover between two parent molecules by cutting and recombining ring substructures. Ring crossover performs a ring cut specifically designed to target ring structures within the molecule. The ring-cut operation cuts the molecule along two different ring patterns, selected randomly. One of the ring patterns checks for a specific arrangement of four consecutive ring atoms, and the other pattern checks for a ring atom connected to two other ring atoms with a single bond. If a suitable ring pattern is found, it cuts the molecule along that pattern, resulting in two fragments. On the other hand, non-ring crossover cuts a single bond, meaning it is not part of a cyclic (ring) structure within the molecule. The obtained fragments from both parents are recombined to create new molecules by applying predefined reaction SMARTS patterns. These operations are repeated for validity to ensure that the resulting molecules meet structural and size constraints.

B.2. Mutation

The mutation is a random change that is introduced to the genetic information of some individuals. This step adds diversity to the population and helps explore new regions of the solution space. In this work, we employ seven different mutation processes and randomly select one of these mutations to modify the offspring molecules slightly. The operations consist of atom and bond deletions, appending new atoms, inserting atoms between existing ones, changing bond orders, deleting cyclic bonds, adding cyclic rings, and altering atom types.

1. Deletion of atom: it selects one of five deletion SMARTS patterns, each representing the removal of a specific number of atoms or bonds. These patterns include the removal of a single atom, a single bond, a bond with two attached atoms, and bonds with multiple attached atoms. The selected pattern is applied to the molecule, deleting the specified atom(s) or bond(s).
2. Appending atom: it introduces a new atom to the molecule. The type of atom (e.g., C, N, O) and the type of bond (single, double, or triple) are chosen based on predefined probabilities. The function then generates a reaction SMARTS pattern to append the selected atom to the molecule, forming a new bond.
3. Inserting atom: it inserts a new atom between two existing atoms in the molecule. Similar to the appending atom, it selects the type of atom and bond based on predefined probabilities and generates a reaction SMARTS pattern to insert the atom.
4. Changing bond order: it randomly selects one of four SMARTS patterns, each representing a change in the bond order between two atoms. These patterns include changing a single bond to a double bond, a double bond to a triple bond, and vice versa.
5. Deletion of cyclic bond: it deletes a bond that is a part of a cyclic structure within the molecule. The SMARTS pattern represents the breaking of a cyclic bond while retaining the atoms connected by the bond.
6. Adding ring: it introduces a new cyclic ring into the molecule by selecting one of four SMARTS patterns, each representing the formation of a specific ring type. These patterns create different types of cyclic structures within the molecule.
7. Changing atom: it randomly selects two types of atoms from a predefined list and generates a SMARTS pattern to change one atom into another. This operation modifies the atom type within the molecule.

C. Hyperparameter Setup for Baseline Methods

In this subsection, we present detailed descriptions for hyperparameter tuning of baselines. For hyperparameters that affect the sample efficiency, such as population size, we have searched for the proper hyperparameters following the guidelines suggested by Gao et al. (2022a). In detail, we tune Mol GA and GEGL on the average AUC Top-10, the main performance metric, from 3 independent runs of two oracles, `zaleplon_mpo` and `perindopril_mpo`. The best configurations are used in the main experiments.

Mol GA. As mentioned in Section 5.2, we set the offspring size as 5, the most crucial hyperparameter, according to Tripp & Hernández-Lobato (2023). Then, we searched the starting population size in [100, 200, 500, 1000] and the population size [100, 200, 500]. As shown in Figure 5, we found the best configuration to be 500 and 100 for the starting population size and the population size, respectively.

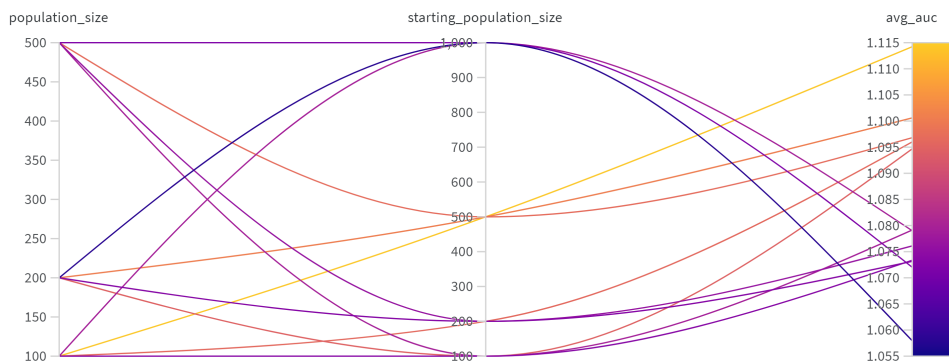


Figure 5. Hyperparameter tuning results for Mol GA

GEGL. In GEGL, the policy sampling size is set as the expert sampling size, and both priority queue sizes (denoted as ‘num_keep’) are the same in the original implementation. Thus, we searched the expert sampling size in [64, 128, 512] and the priority queue size in [128, 512, 1024]. Originally, they were set as 8192 and 1024, which are improper to the sample efficient setting. For the training batch size, we use 64, which is the same as ours. We use the pre-trained policy provided in the original code and adapt the setup of the rest of the hyperparameters, including mutation rate, learning rate, and the number of training loops.

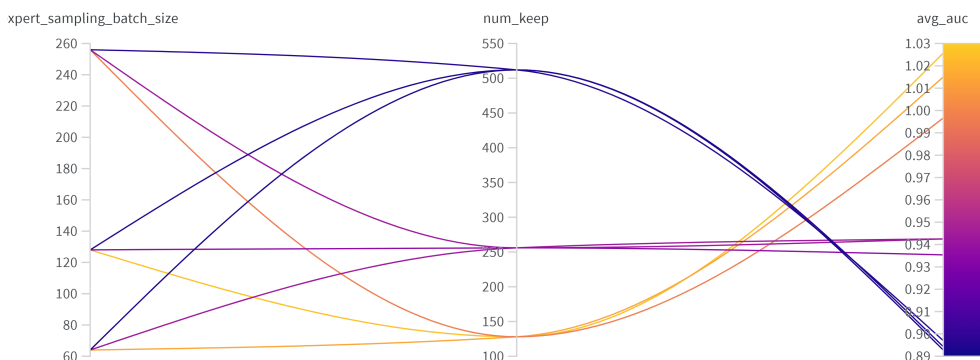


Figure 6. Hyperparameter tuning results for GEGL

D. Additional Results

D.1. Rank with various metrics

According to the PMO benchmark, we also provide the rank of each method with various metrics. The results in Table 5 show that Genetic GFN achieves the first place in total, not only in the AUC Top-10.

Table 5. The rank of 10 methods based on various performance metrics

Methods	AUC Top-1	AUC Top-10	AUC Top-100	Avg. Top-1	Avg. Top-10	Avg. Top-100	Mean
Genetic GFN (Ours)	1	1	1	1	1	1	1
Mol GA	2	2	2	4	3	2	2.50
SMILES-REINVENT	3	3	3	3	2	3	2.83
SELFIES-REINVENT	6	5	4	5	5	4	4.83
GP BO	5	4	5	6	6	5	5.17
SMILES-LSTM-HC	4	7	9	2	4	6	5.33
Graph GA	7	6	6	7	7	7	6.67
STONED	8	8	7	8	8	8	7.83
SMILES GA	9	9	10	9	9	10	9.33
SynNet	10	10	8	10	10	9	9.50

D.2. Results for Diversity and Synthesizability

We report the diversity and synthetic accessibility (SA) score of Top-100 molecules on each oracle.

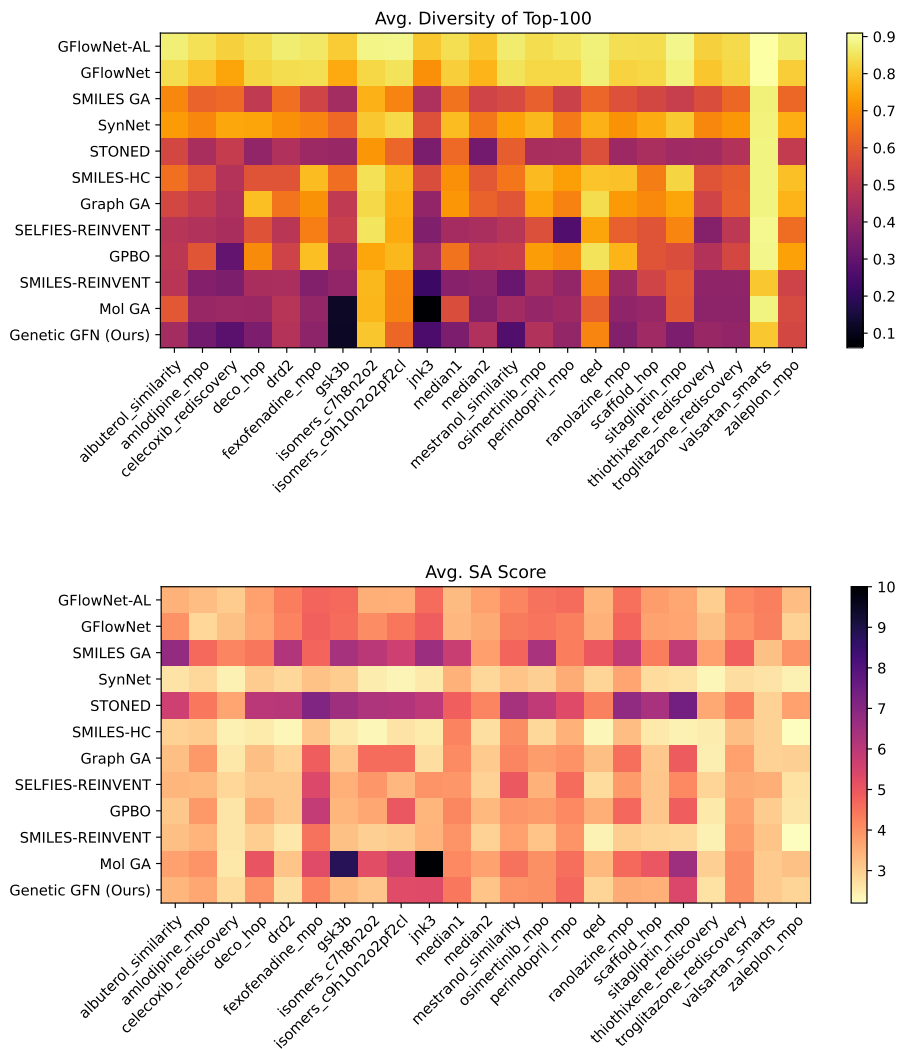


Figure 7. The average SA score of Top-100 molecules (\downarrow)

D.3. Comparison with Other GFlowNets

We provide the results of GFlowNet (Bengio et al., 2021a) and GFlowNet-AL (Jain et al., 2022). The experiments are conducted based on the implementation of the PMO benchmark.

Table 6. The average and standard deviation of AUC Top-10 of GFlowNet variants.

Oracle	GFlowNet	GFlowNet-AL	Genetic GFN
albuterol_similarity	0.459 ± 0.028	0.382 ± 0.010	0.949 ± 0.010
amlodipine_mpo	0.437 ± 0.007	0.428 ± 0.002	0.761 ± 0.019
celecoxib_rediscovery	0.326 ± 0.008	0.263 ± 0.009	0.802 ± 0.029
deco_hop	0.587 ± 0.002	0.582 ± 0.001	0.733 ± 0.109
drd2	0.601 ± 0.055	0.480 ± 0.075	0.974 ± 0.006
fexofenadine_mpo	0.700 ± 0.005	0.689 ± 0.003	0.856 ± 0.039
gsk3b	0.666 ± 0.006	0.589 ± 0.009	0.881 ± 0.042
isomers_c7h8n2o2	0.468 ± 0.211	0.791 ± 0.024	0.969 ± 0.003
isomers_c9h10n2o2pf2cl	0.199 ± 0.199	0.576 ± 0.021	0.897 ± 0.007
jnk3	0.442 ± 0.017	0.359 ± 0.009	0.764 ± 0.069
median1	0.207 ± 0.003	0.192 ± 0.003	0.379 ± 0.010
median2	0.181 ± 0.002	0.174 ± 0.002	0.294 ± 0.007
mestranol_similarity	0.332 ± 0.012	0.291 ± 0.005	0.708 ± 0.057
osimertinib_mpo	0.785 ± 0.003	0.787 ± 0.002	0.860 ± 0.008
perindopril_mpo	0.434 ± 0.006	0.423 ± 0.006	0.595 ± 0.014
qed	0.917 ± 0.002	0.904 ± 0.002	0.942 ± 0.000
ranolazine_mpo	0.660 ± 0.004	0.626 ± 0.005	0.819 ± 0.018
scaffold_hop	0.464 ± 0.003	0.461 ± 0.002	0.615 ± 0.100
sitagliptin_mpo	0.217 ± 0.022	0.180 ± 0.012	0.634 ± 0.039
thiothixene_rediscovery	0.292 ± 0.009	0.261 ± 0.004	0.583 ± 0.034
trogliatzone_rediscovery	0.190 ± 0.002	0.183 ± 0.001	0.511 ± 0.054
valsartan_smarts	0.000 ± 0.000	0.000 ± 0.000	0.135 ± 0.271
zaleplon_mpo	0.353 ± 0.024	0.308 ± 0.027	0.552 ± 0.033
Sum	9.917	9.929	16.213

Table 7. Performance of GFlowNet variants.

	GFlowNet	GFlowNet-AL	Genetic GFN (Ours)
AUC Top-1	10.957	11.032	16.527
AUC Top-10	9.917	9.929	16.213
AUC Top-100	8.416	8.064	15.516
Diversity	0.816	0.846	0.432

D.4. Results for Ablation Studies

Table 8. The full results of Table 2.

Oracle	Genetic GFN			GEGL
	Ours	w/o GS	w/o KL	
albuterol_similarity	0.949 ± 0.010	0.942 ± 0.007	0.946 ± 0.012	0.842 ± 0.019
amlodipine_mpo	0.761 ± 0.019	0.686 ± 0.046	0.705 ± 0.029	0.626 ± 0.018
celecoxib_rediscovery	0.802 ± 0.029	0.804 ± 0.068	0.810 ± 0.022	0.699 ± 0.041
deco_hop	0.733 ± 0.109	0.746 ± 0.088	0.664 ± 0.014	0.656 ± 0.039
drd2	0.974 ± 0.006	0.962 ± 0.013	0.975 ± 0.004	0.898 ± 0.015
fexofenadine_mpo	0.856 ± 0.039	0.818 ± 0.010	0.822 ± 0.014	0.769 ± 0.009
gsk3b	0.881 ± 0.042	0.889 ± 0.048	0.892 ± 0.062	0.816 ± 0.027
isomers_c7h8n2o2	0.969 ± 0.003	0.939 ± 0.035	0.969 ± 0.003	0.930 ± 0.011
isomers_c9h10n2o2pf2cl	0.897 ± 0.007	0.884 ± 0.025	0.881 ± 0.020	0.808 ± 0.007
jnk3	0.764 ± 0.069	0.799 ± 0.055	0.627 ± 0.113	0.580 ± 0.086
median1	0.379 ± 0.010	0.369 ± 0.007	0.367 ± 0.018	0.338 ± 0.016
median2	0.294 ± 0.007	0.284 ± 0.009	0.296 ± 0.012	0.274 ± 0.007
mestranol_similarity	0.708 ± 0.057	0.666 ± 0.086	0.695 ± 0.061	0.599 ± 0.035
osimertinib_mpo	0.860 ± 0.008	0.854 ± 0.013	0.851 ± 0.013	0.832 ± 0.005
perindopril_mpo	0.595 ± 0.014	0.560 ± 0.022	0.610 ± 0.035	0.537 ± 0.015
qed	0.942 ± 0.000	0.942 ± 0.000	0.942 ± 0.000	0.941 ± 0.001
ranolazine_mpo	0.819 ± 0.018	0.808 ± 0.024	0.818 ± 0.020	0.730 ± 0.011
scaffold_hop	0.615 ± 0.100	0.608 ± 0.062	0.583 ± 0.029	0.531 ± 0.010
sitagliptin_mpo	0.634 ± 0.039	0.509 ± 0.065	0.644 ± 0.036	0.402 ± 0.024
thiothixene_rediscovery	0.583 ± 0.034	0.576 ± 0.038	0.605 ± 0.011	0.515 ± 0.028
trogliatzone_rediscovery	0.511 ± 0.054	0.540 ± 0.042	0.517 ± 0.058	0.420 ± 0.031
valsartan_smarts	0.135 ± 0.271	0.000 ± 0.000	0.166 ± 0.332	0.119 ± 0.238
zaleplon_mpo	0.552 ± 0.033	0.551 ± 0.027	0.543 ± 0.027	0.492 ± 0.021
Sum	16.213	15.736	15.928	14.354

Table 9. Results of ablation studies.

	Genetic GFN			GEGL
	Ours	w/o GS	w/o KL	
AUC Top-1	16.527	16.070	16.251	15.060
AUC Top-10	16.213	15.736	15.928	14.354
AUC Top-100	15.516	15.030	15.188	13.142
Diversity	0.453	0.479	0.442	0.540

Table 10. Performance of Genetic GFN with SELFIES generations.

Oracle	SELFIES REINVENT	SELFIES Genetic GFN
albuterol_similarity	0.867 ± 0.025	0.918 ± 0.031
amlodipine_mpo	0.621 ± 0.015	0.711 ± 0.029
celecoxib_rediscovery	0.588 ± 0.062	0.578 ± 0.049
deco_hop	0.638 ± 0.016	0.631 ± 0.020
drd2	0.953 ± 0.009	0.971 ± 0.005
fexofenadine_mpo	0.740 ± 0.012	0.797 ± 0.012
gsk3b	0.821 ± 0.041	0.900 ± 0.042
isomers.c7h8n2o2	0.873 ± 0.041	0.952 ± 0.017
isomers.c9h10n2o2pf2cl	0.844 ± 0.016	0.879 ± 0.031
jnk3	0.624 ± 0.048	0.675 ± 0.140
median1	0.353 ± 0.006	0.351 ± 0.034
median2	0.252 ± 0.010	0.263 ± 0.014
mestranol_similarity	0.589 ± 0.040	0.680 ± 0.076
osimertinib_mpo	0.819 ± 0.005	0.849 ± 0.008
perindopril_mpo	0.533 ± 0.024	0.551 ± 0.015
qed	0.940 ± 0.000	0.942 ± 0.000
ranolazine_mpo	0.736 ± 0.008	0.785 ± 0.013
scaffold_hop	0.521 ± 0.014	0.531 ± 0.020
sitagliptin_mpo	0.492 ± 0.055	0.590 ± 0.018
thiothixene_rediscovery	0.497 ± 0.043	0.527 ± 0.036
troglitazone_rediscovery	0.342 ± 0.022	0.387 ± 0.087
valsartan_smarts	0.000 ± 0.000	0.000 ± 0.000
zaleplon_mpo	0.509 ± 0.009	0.518 ± 0.016
Sum	14.152	14.986
Diversity	0.555	0.528

D.5. Genetic GFN with SELFIES generation

As our method employs a string-based sequence generation model, it is applicable to SELFIES representation. Following the same procedure and setup described in Section 3 and Section 5.1. The results in Table 10 demonstrate that Genetic GFN significantly outperforms SELFIES-REINVENT by achieving 14.986 compared to 14.152, not only the other high-ranked method, GP BO (14.264). Notably, our achieves the higher AUC Top-10 than SELFIES-REINVENT in 19 oracles.

D.6. Experiments with Varying Hyperparameters

In this subsection, we verify the robustness of Genetic GFN for differing hyperparameter setups. We conduct experiments by varying the number of GA generation (refining loops), offspring size, and the number of training inner loops. The results show that our results are robust to each hyperparameter setup by achieving similar or better performance compared to Mol GA in all tested configurations.

Table 11. Ablation studies for the number of GA generation. ‘ $\times 0$ ’ stands for the results of TB loss training without GA explorations.

Oracle	$\times 0$	$\times 1$	$\times 2$	$\times 3$
AUC Top-1	16.070	15.968	16.527	16.040
AUC Top-10	15.738	15.615	16.213	15.735
AUC Top-100	15.030	14.909	15.516	15.074
Diversity	0.479	0.470	0.432	0.440

Table 12. Results by varying the offspring size.

Oracle	4	8	16	32
AUC Top-1	16.174	16.527	15.984	15.963
AUC Top-10	15.846	16.213	15.669	15.621
AUC Top-100	15.175	15.516	14.977	14.858
Diversity	0.458	0.432	0.452	0.437

Table 13. Results by varying the number of training inner loops.

Oracle	$\times 4$	$\times 8$	$\times 16$
AUC Top-1	16.125	16.527	16.049
AUC Top-10	15.768	16.213	15.717
AUC Top-100	15.175	15.516	14.977
Diversity	0.423	0.432	0.511